Pergamon

Int. J. Solids Structures Vol. 32, No. 2, pp. 235–249, 1995

0020–7683/95 $9.50 + .00

0020–7683(94)00105–7

ANALYSIS OF THIN-WALLED ANISOTROPIC FRAMES BY THE DIRECT STIFFNESS METHOD

EMMANUEL COFIE† and LAWRENCE C. BANK
Department of Civil Engineering, The Catholic University of America, Washington, DC 20064, U.S.A.

(*Received* 28 *July* 1993; *in revised form* 29 *April* 1994)

Abstract—The stiffness matrix for a one-dimensional beam element for use in a direct stiffness matrix method for analysing thin-walled anisotropic frames is presented in this paper. Thin-walled beams are widely used as structural components and stiffeners in aerospace and civil engineering applications. The stiffness matrices for two 2-noded 12 degrees of freedom beam elements, one of which accounts for warping and anisotropic coupling only and called a "warping superelement", and the other a "non-warping element", are developed numerically. The warping superelement is used in the region of the beam where warping is considered critical. The length of this region, which is dependent on the geometric and mechanical properties of the beam cross-section, is determined using a technique that utilizes equivalent one-dimensional mechanical properties of the composite material panels in the cross-section. The non-warping element is used outside of this critical region. Numerical examples of a thin-walled space frame structure are presented to demonstrate the use of the beam model. Results obtained using the proposed model are compared with numerical results obtained from 2-D finite element analysis.

INTRODUCTION

In recent years, thin-walled anisotropic composite material profile sections have been developed for structural components in the civil, mechanical and aerospace industry. Light weight, high resistance to corrosion, high strength to stiffness ratios and aeroelastic tailoring capabilities are some of the reasons for the development. Often it is necessary to analyse frameworks consisting of an assemblage of open-section thin-walled structural members. In most commercial structural analysis computer codes only St Venant torsion is considered in the beam models. It is a well known fact, however, that warping torsion is significant in constrained beam members and should be taken into account. The presence of warping (Vlasov, 1961; Gjelsvik, 1981; Cofie, 1993a) tends to present a difficulty in the analysis of thin-walled isotropic structures. The problem becomes even more complex with anisotropic structures. The presence of anisotropic coupling responses (Bank 1990; Cofie, 1993a,b; Bank and Cofie, 1992, 1993), normally not encountered in isotropic thin-walled structures becomes a major concern. These anisotropic coupling responses result in behaviors not observed in isotropic structures. The application of, say, an in-plane load not only generates an in-plane response (observed in isotropic structures) but also an out-of-plane response of the structure. This out-of-plane response presents a problem when one considers the concept of plane frame or beam analysis based on the assumption that the structure remains in a two-dimensional plane, valid for isotropic structures. Use of a two-dimensional model is not possible. In order, therefore, to accurately analyse a thin-walled anisotropic composite frame, one needs to utilize a model that predicts responses in three-dimensional space, rather than that which predicts responses in a two-dimensional plane. Most traditional structural analysis codes developed for isotropic materials in which coupling is known to be absent, cannot be used to analyse anisotropic thin-walled composite structures. Due to the presence of coupling effects, the analysis of thin-walled anisotropic structures are currently usually performed using finite element packages that utilize either composite plate or shell elements (NASTRAN, 1986; NISA, 1990), which demand large storage space and tend to be very expensive.

† Now at: FHWA, Turner-Fairbank Highway Research Center, McLean, Virginia, U.S.A.

Prior attempts made at developing one-dimensional beam models based on the finite element formulation for the analysis of thin-walled anisotropic structures, to account for warping and anisotropic coupling, have included additional degrees of freedom (d.o.f.) to the "normal" 6 d.o.f. to account for the warping related deformation. Pioneering work on anisotropic structures was carried out by Mansfield and Sobey (1979) on a general anisotropic two cell thin-walled tube subjected to longitudinal tension and torsion. Rehfield (1985) presented a simplified beam model in which a 7×7 stiffness matrix relating the generalized internal forces to the generalized strains was developed, with two non-classical influences, transverse shear deformation and torsion-related warping included. The literature pertaining to the development of one-dimensional beam models for the analysis of thin-walled anisotropic composite structures based on the Vlasov theory is limited. Bauld and Tzeng (1984) presented a linear theory based on an extension of the Vlasov theory to anisotropic structures, in which the presence and effects of coupling were examined. Gupta *et al.* (1985) developed a one-dimensional 16 d.o.f. beam model for the analysis of anisotropic thin-walled composite structures without any restrictions on the lamination scheme. Hong and Chopra (1986) extended a one-dimensional 15 d.o.f. beam model developed by Sivaneri and Chopra (1984) for isotropic rotor blades, to enable the treatment of composite rotor blades. Stemple and Lee (1988) presented a one-dimensional beam finite element model in which additional nodes were introduced to account for warping. Nagarajan and Zak (1985) and Zak (1987), in addition to discussing the limitations of existing finite element models, also presented a beam model for the analysis of orthotropic composite beams without warping. Chandra and Chopra (1991) using a Vlasov type linear theory presented a 14 d.o.f. beam model for the analysis of composite I-beams with elastic couplings. The effects of warping were included directly by extending the Vlasov differential equations of torque equilibrium to the classical lamination theory of composite plates. In an effort to provide a simplified one-dimensional beam theory for preliminary design, Bank (1990) presented a modified beam theory for the analysis of anisotropic thin-walled composite beams. This model was confirmed numerically by Bank and Cofie (1992), and experimentally by Smith and Bank (1992). The objective here was on simplicity and easy desk-top calculations. Bank and Cofie (1992) in another paper presented a more realistic model of a thin-walled composite beam. The distinctive feature of these studies was their ability to isolate and estimate theoretically, the out-of-plane displacements associated with thin-walled composite beams, and further verify them by 2-D finite element results and experimental results. Warping was not considered, since torsional loading was not considered in these models.

The current paper presents two 2-noded 12 d.o.f. beam elements; one is called a "warping superelement" and the other is called a "non-warping element" for the analysis of thin-walled anisotropic framed structures to include the effects of warping and anisotropy. The numerical development of the stiffness matrices is outlined and their application to the analysis of anisotropic thin-walled framed structures is described.

STIFFNESS MATRIX DEVELOPMENT

To account for the effects of warping and anisotropy, the model described by Cofie (1993a) for isotropic beam elements was extended to include anisotropy and used for the development of the element stiffness matrix. Numerical techniques were used as opposed to variational methods (Cofie, 1993b). The beam was divided into two regions, a warping region, and a non-warping region. The element in the warping region is called a "warping superelement", because the terms in the stiffness matrix directly include the effects of warping. The concept of warping and non-warping regions is due to the well known fact that thin-walled sections develop non-uniform warping related stresses at restrained ends and load application points of the beam (Gjelsvik, 1981) which tend to decay at an exponential rate. Consequently, the region close to the restraints, called the "critical region", can be assumed to be under non-uniform torsion while those further away from the restraints can be assumed to be subjected to pure torsion only. The length of the critical

region establishes the governing criterion for numerically generating the element stiffness matrices. Two-dimensional finite element discretizations were used to assemble the two 12×12 element stiffness matrices for the anisotropic thin-walled beam section. The force method of analysis where unit loads are applied to the free end of the cantilever beam was used and the stiffness matrix obtained from the numerical inversion of the flexibility matrix. This approach allows for warping displacements to be clearly specified. Prior to assembling the element stiffness matrices, the boundaries of the different regions within the beam member and the length of the warping region (the critical length) are determined.

The critical length

The estimation of the length of the warping influenced region (critical region) of the anisotropic beam is based on an approximate technique, proposed by Cofie (1993a) for isotropic beams. In that paper the torsional stiffness term, based on the Vlasov theory is given as,

$$S_t = \left[1 + \frac{\tanh(\alpha L)}{\alpha L - \tanh(\alpha L)}\right]\frac{GJ}{L}, \tag{1}$$

where

$$\alpha = \sqrt{\frac{GJ}{EI_{\Omega\Omega}}}$$

$$J = \int_s t^3 \, ds$$

$$I_{\Omega\Omega} = \int_A 4(\omega_0 - \omega)^2 \, dA \tag{2}$$

and E is the Young's modulus; G, the shear modulus; J the St Venant torsion constant; $I_{\Omega\Omega}$ the warping constant; ω and ω_0, the sectorial areas; A, the cross-sectional area; and L, the length of the beam element. Equation (1) consists of two expressions, one representing the contribution of the St Venant torsional stiffness and the other the warping stiffness. Additionally it can be seen that the expression related to the warping effects is a function of the factor αL, and that this expression decays rapidly as αL increases (or as L increases), as one moves away from the warping restrained end of the beam. Another interpretation of this expression is that, at points very close to the restrained end, the beam tends to develop a Vlasov stiffness, while at points further away, the beam tends to approach a St Venant torsional stiffness. In light of this behavior, it is assumed that elements close to the torsionally restrained end of the beam develop Vlasov stiffness, while elements further away will develop St Venant stiffness.

At this point the typical thin-walled beam can be considered to consist of two regions: a region that contains the warping superelement and a region that contains the conventional beam elements. The only difference between the elements in these two regions is with respect to their torsional stiffnesses. The element in the warping region is called a superelement because its torsional stiffness terms directly account for warping, in addition to St Venant torsion. One can visualize the concept as one of having to condense the warping (non-uniform torsion) response of this entire region into one big element which is called the "superelement" that can be used in a linear analysis. It should be noted here that only a single warping superelement can be used in the warping region (called the "critical region"), whereas as many elements as desirable can be used outside of the critical region. This is due to the fact that the torsional behavior in the critical region is non-uniform, whereas the region outside of the critical region exhibits uniform torsional behavior (St Venant torsion). In addition to restrained ends, warping effects are known to be significant in the regions around the point of application of a torsional load, according to Vlasov (1961), unless free

warping is allowed to take place at the point. Warping superelements may therefore be required at these points in addition to the beam ends.

The term "superelement" used in this paper differs from that used in some commercial finite element codes. The term "superelement" is used in most finite element codes in relation to substructuring, where the full structure is divided into modules called substructures or superelements, each substructure capable of being analysed independently using the same theory (NASTRAN, 1986). The term "superelement" in this study refers to an element with reduced d.o.f. at the nodes and whose responses are only obtained at the nodes at the ends of the superelement. In order to obtain responses of intermediate points within the superelement, a separate analysis must be used. It should be noted that the superelement developed in this work cannot be simply obtained by using a superelement substructuring technique in a finite element code.

The length of the critical region, which defines the length of the warping superelement is dependent on the geometrical and mechanical properties of the section. The torsional stiffness term of eqn (1) can be written in terms of the contributing terms as

$$S_t = S_v + S_w, \tag{3}$$

where S_v and S_w are the contributions from the St Venant and warping torsion, respectively. For the case of pure torsion, the torsional stiffness term is given by

$$S_v = \frac{GJ}{L}. \tag{4}$$

The ratio of these two torsional stiffnesses, eqns (3) and (4), denoted by Δ, can be written as

$$\Delta = \frac{S_v}{S_t} = \left[1 - \frac{\tanh(\alpha L)}{\alpha L}\right]. \tag{5}$$

At this point a threshold value of this ratio can be defined, Δ_c. Beyond Δ_c, the beam is considered to be under St Venant torsion. This threshold value defines the length of the critical region and in effect the length of the warping superelement. Writing eqn (5) in inequality form gives

$$\tanh(\alpha L) \leqslant [1 - \Delta_c](\alpha L). \tag{6}$$

Solving the above transcendental eqn (6) gives the length of the critical region, the point beyond which the assumption of the pure St Venant torsional stiffness approximation will be acceptable. The functions on either side of the inequality (6) are plotted as a function of (αL) in Fig. 1. The plot shows the two expressions on each side of eqn (6) for different values of Δ. Points to the right of the intersection of the two curves give acceptable solutions to eqn (6). Notice the shape of the curve of the function on the left hand side of the inequality. It has a nonlinear and a linear part. The nonlinear part of the curve represents the region of the beam where the warping effect is critical, while the linear part represents the region of the beam where the warping effect is insignificant. This implies that beyond a certain point on the beam, the effects of warping are so insignificant as to not affect the overall torsional response of the structure. In practical terms, increasing the value of Δ, which corresponds to a point further down the linear part of the left hand side curve, is equivalent to increasing the degree of accuracy of the results. Efficiency and cost will however impose practical limitations on the degree of accuracy and thus on Δ. Typically, acceptable values of Δ_c are determined from the linear region of the curve. For any given Δ, the corresponding value of (αL), which is unique, can be obtained from the graph. The advantage of using Fig. 1 is that it is a universal figure and can therefore be used to determine the critical length of any arbitrarily shaped thin-walled open section. With the

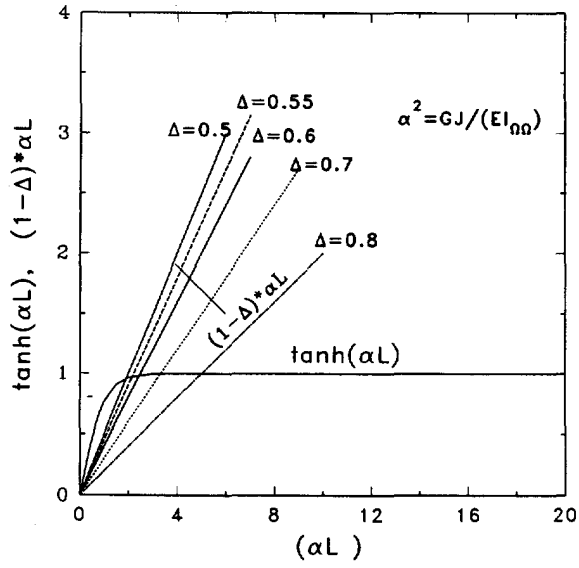

Fig. 1. Ratio of stiffness.

value of α obtained from eqn (2), the length of the superelement can be determined. The larger the value of Δ, the longer the length of the warping superelement. Since only a single superelement can be used in the critical region, it is advantageous to use the smallest length possible, without sacrificing too much accuracy. Moreover, since responses of points within the superelement have to be obtained from a separate analysis, it is in the interest of the analyst to choose a warping superelement that is as small as possible, so as to obtain as much information as possible on the response of the beam at this stage of the analysis. Figure 1 shows that a value of Δ_c of 0.5, cuts the curve just at the beginning of the linear region. This gives a value of $\alpha L \approx 2$ from eqn (6). The length of the critical region and thus the length of the superelement (L_c) is therefore

$$L_c = \frac{2}{\alpha}. \tag{7}$$

Equation (7), which was developed for isotropic beams is extended to account for anisotropic beams. To simplify and thereby reduce the complexity of the derivations involved, basic assumptions pertaining to the behavior of anisotropic thin-walled structures, parallel to those used in isotropic thin-walled structures are made. The basis for the assumptions is due, in part, to the fact that in the one-dimensional analysis of laminated composite beams, the use of effective stiffness properties of the laminate along the beam axis to characterize the one-dimensional behavior of the beam is common (Vinson and Sierakowski, 1987; Whitney, 1987). In addition, Noor *et al.* (1991) and Bank (1990) have demonstrated that sufficiently accurate results could be obtained using effective properties. For the laminates discussed in this paper effective one-dimensional mechanical properties were derived. These effective properties were then used to determine the approximate length of the critical region for anisotropic thin-walled structures.

Effective one-dimensional properties

Consider the anisotropic thin-walled beam shown in Fig. 2 constructed from laminated panels and subjected to a twist (torsional deformation). Define the laminate's axes as the 1–2 axes with the 1-axis parallel to the beam x-axis (longitudinal axis). Notice that the orientation of the 2-axis depends on whether the panel is parallel to the y- or z-axis. In order to ensure clarity the subscript i is used to denote the ith panel ($i = t, c, b$ for top, center and bottom). Following assumptions similar to those made in isotropic thin-walled

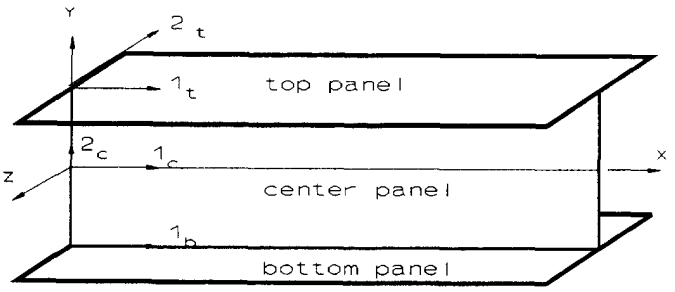

Fig. 2. Local and global coordinate system for a typical beam element.

structures subjected to torsional deformation the only non-zero strain component developed in the section is the shear strain ε_6. The components of strain in the normal directions (i.e. ε_1 and ε_2) are zero, where 1 and 2 refer to the 1- and 2-axis of the panel, respectively. From classical lamination theory of composite plates (Tsai and Hahn, 1980) the stress–strain relationship of the ith panel in terms of its off-axis engineering constants can be written as

$$\{\varepsilon\} = [S]\{\sigma\} \quad \text{or} \quad \begin{aligned} 0 &= \left[\frac{1}{E_1}\sigma_1 - \frac{\nu_{21}}{E_1}\sigma_2 + \frac{\nu_{61}}{E_1}\sigma_6\right]_i \\ 0 &= \left[-\frac{\nu_{12}}{E_2}\sigma_1 + \frac{1}{E_2}\sigma_2 + \frac{\nu_{62}}{E_2}\sigma_6\right]_i \\ \varepsilon_6 &= \left[\frac{\nu_{16}}{E_6}\sigma_1 + \frac{\nu_{26}}{E_6}\sigma_2 + \frac{1}{E_6}\sigma_6\right]_i \end{aligned} \tag{8}$$

where E_1 and E_2 are the in-plane longitudinal and transverse moduli in the 1–1 and 2–2 directions, E_6 is the in-plane shear modulus, ν_{12} and ν_{21} are the in-plane Poisson's ratios, ν_{16} and ν_{26} are the in-plane normal coupling coefficients, ν_{61} and ν_{62} are the in-plane shear coupling coefficients, ε_1, ε_2 and ε_6 are the normal and shear strains, and σ_1, σ_2 and σ_6 are the normal and shear stresses. Due to the presence of the normal–shear coupling ratios, the normal stresses σ_1 and σ_2 are non-zero. Solving the first two rows of eqn (8) in terms of the shear stress σ_6, the non-zero stresses are obtained as

$$\sigma_{1_i} = \left[\frac{\nu_{62}\nu_{21} + \nu_{61}}{\nu_{21}\nu_{12} - 1}\right]_i \sigma_{6_i}, \tag{9}$$

$$\sigma_{2_i} = \left[\frac{\nu_{12}\nu_{61} + \nu_{62}}{\nu_{21}\nu_{12} - 1}\right]_i \sigma_{6_i}. \tag{10}$$

Substituting eqns (9) and (10) into the last row of eqn (8) results in the following expression which can be written as

$$\varepsilon_{6_i} = \left[1 - \frac{\nu_{16}(\nu_{62}\nu_{21} + \nu_{61}) + \nu_{26}(\nu_{61}\nu_{12} + \nu_{62})}{1 - \nu_{21}\nu_{12}}\right]_i \frac{\sigma_{6_i}}{E_{6_i}}, \tag{11}$$

$$\sigma_{6_i} = \beta E_6 \varepsilon_{6_i}, \tag{12}$$

where β is called the "transformation parameter" and is defined as

$$\beta = \frac{1}{\left[1 - \dfrac{\nu_{16}(\nu_{62}\nu_{21} + \nu_{61}) + \nu_{26}(\nu_{61}\nu_{12} + \nu_{62})}{1 - \nu_{21}\nu_{12}}\right]}. \tag{13}$$

The terms in the expression for β contain coupling and Poisson coefficients of panel i and are different for each panel. For isotropic thin-walled beams $\beta = 1$. β has a scaling effect on the effective in-plane shear modulus E_6 of the panel. It is sensitive to the degree of anisotropy of the panel. β transforms the effective shear modulus of the panel, E_6, into an equivalent one-dimensional shear modulus ($G_{1\text{-D}}$). A new term, $G_{1\text{-D}}$, is introduced to represent this equivalent one-dimensional shear modulus for the panel, defined as

$$G_{1\text{-D}} = \beta E_{6_i}. \tag{14}$$

For a unidirectional or cross-ply laminate the normal and shear coupling coefficients are all zero. β becomes unity and eqn (14) yields the effective shear modulus, E_6. In the case of the one-dimensional longitudinal modulus, the Poisson effects are typically small and can be neglected (Gjelsvik, 1981) and the one-dimensional longitudinal modulus, $E_{1\text{-D}}$ is assumed to be equal to the in-plane modulus, E_1. Having obtained $G_{1\text{-D}}$ and $E_{1\text{-D}}$, the length of the critical region is determined using the same procedure outlined for isotropic sections given by eqn (7). For the case of a beam in which the panels have different $G_{1\text{-D}}$'s and $E_{1\text{-D}}$'s, a transformed section method similar that used for nonhomogeneous materials is used (Timoshenko, 1965) with α now given as

$$\alpha = \sqrt{\frac{\sum G_{1\text{-D}} J^{\mathrm{t}}}{\sum E_{1\text{-D}} I^{\mathrm{t}}_{\Omega\Omega}}} \tag{15}$$

where the superscript t refers to the transformed section.

The "warping superelement" stiffness matrix

To obtain the warping superelement stiffness matrix, a beam element of length equal to the critical length, L_c is modeled using a finite element code with laminated composite plate (or shell) elements. The beam cross-section is modeled with a number of elements which gives many nodes (and d.o.f.) at each station along the length of the beam. Because the cross-section of the beam has more than one node, the kinematic and static conditions at these nodes have to be described in such a way as to effectively simulate or approximate the one-dimensional beam model. This was achieved using master-slave node concepts (Norris *et al.*, 1976), in which kinematic constraints at the nodes were coupled through the use of multi-point constraint (MPC) equations or rigidlinks. One advantage gained from using the master-slave node concept was that loads could be applied directly to the end of the beam via the master node. At the fixed end of the beam, all the displacements of the slave nodes were coupled to the master node and all six displacements at the master node set to zero. This description ensured zero displacements for all d.o.f. and therefore met the condition of restrained warping. At the free end of the beam the axial displacements of the slave nodes were intentionally uncoupled from the master node. This allowed unconstrained displacement in the longitudinal direction of the nodes on the cross-section, thus allowing for free warping of the cross-section. The load (i.e. stress-resultant) was applied to the master node. Six cases were run corresponding to the six stress resultants at the end of the beam, each case generating one column of the 6×6 flexibility matrix. The element stiffness matrix was then obtained from the numerical inversion of the flexibility matrix. The difference between this element stiffness matrix developed here and that of an isotropic beam is that the element stiffness matrix of the anisotropic beam is fully populated, whereas most of the off-diagonal terms of the element stiffness matrix of the isotropic beam are zero. In order to get a sense of the effects of the anisotropic coupling coefficients on the

element stiffness matrix, a schematic representation of the full stiffness matrix of the anisotropic beam element is shown in eqn (16):

$$\begin{bmatrix} x & a & a & a & a & a & x & a & a & a & a & a \\ a & x & a & a & a & x & a & x & a & a & a & x \\ a & a & x & a & x & a & a & a & x & a & x & a \\ a & a & a & x & a & a & a & a & a & x & a & a \\ a & a & x & a & x & a & a & a & x & a & x & a \\ a & x & a & a & a & x & a & x & a & a & a & x \\ x & a & a & a & a & a & x & a & a & a & a & a \\ a & x & a & a & a & x & a & x & a & a & a & x \\ a & a & x & a & x & a & a & a & x & a & x & a \\ a & a & a & x & a & a & a & a & a & x & a & a \\ a & a & x & a & x & a & a & a & x & a & x & a \\ a & x & a & a & a & x & a & x & a & a & a & x \end{bmatrix}. \tag{16}$$

The symbol "x" is used to indicate the non-zero terms in the matrix that also appear as non-zero terms in the isotropic stiffness matrix, and "a" to indicate the anisotropic coupling induced non-zero terms which never appear in the isotropic stiffness matrix. The coupling responses are due to the presence of these non-zero terms.

The "non-warping element" stiffness matrix

The non-warping element stiffness matrix is also obtained numerically following a similar procedure outlined for the warping superelement. Since the "non-warping element" is independent of length, any convenient length can be used. The difference in the numerical determination being that the axial displacements of the slave nodes at both ends of the beam are uncoupled from the master node, thus enabling both ends of the beam to warp.

NUMERICAL EXAMPLES

An example of a three-dimensional frame structure with the structural components labelled Beam 1, Beam 2 and Column 1 shown in Fig. 3 is analysed to demonstrate the use of the proposed model. The material chosen is graphite–epoxy, with orthotropic material properties of $E_{xx} = 181.0$ GPa, $E_{yy} = 10.3$ GPa, $E_{ss} = 7.17$ GPa and $\nu_{xy} = 0.28$. Beam 1, Beam 2, and Column 1 all have the same geometrical shape (I-shaped). The top flange, the web and the bottom flange of the I-shaped sections of the beams or column are referred to as top, center and bottom panels, respectively. The I-shaped sections all have the same cross-sectional dimensions. The top, center and bottom panels are all 30 mm × 2 mm thick. Beam 1 is 800 mm long, with the center panel parallel to the X–Y plane, Beam 2 is 1600 mm long, with the center panel parallel to the Y–Z plane, and Column 1 is 120 mm long, with the center panel parallel to the Y–Z plane.

An identification terminology called the "Composite Structural Identification Pattern" (CSIP), is introduced to describe the ply orientation, lamination stacking sequences and the sequence of the panels forming the cross section of the thin-walled structure (i.e. top, center and bottom panels). Ply orientation is defined relative to the longitudinal axis of the panel being described (where a positive angle represents a counterclockwise rotation). Ply orientations and lamination sequences are enclosed in small square brackets ([ ]), and the CSIP is enclosed in big square brackets. Two examples with different CSIPs (CSIP 1 and CSIP 2) were used to demonstrate the proposed procedure, the accuracy of the results and to illustrate the phenomena of twist of the section without out-of-plane motion, and an out-of-plane motion without a twist, a behavior demonstrated by Bank (1990) and Bank

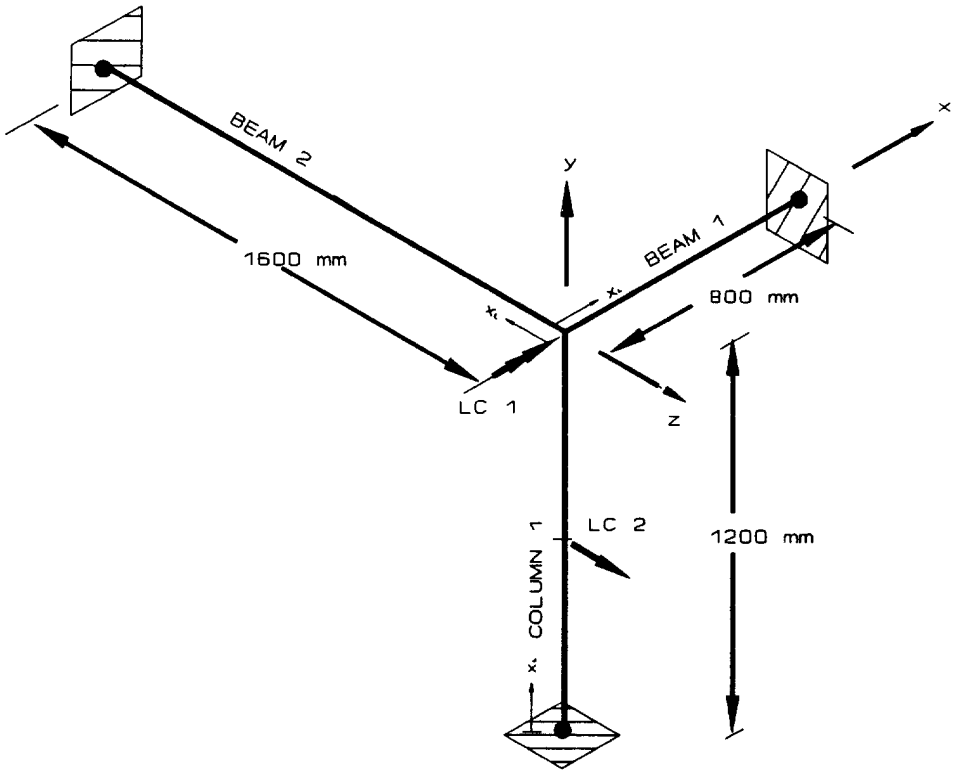

Fig. 3. Anisotropic thin-walled composite space frame.

and Cofie (1992) and later proved experimentally by Smith and Bank (1992) on one-dimensional anisotropic thin-walled beams. For the example presented, only the "significant" responses are illustrated and compared with 2-D finite element results. Significant in this context refers to responses due mainly to anisotropic coupling. Rotations (total twist) are mainly shown because these responses tend to be heavily influenced by restrained warping, and thus the length of the critical region. The CSIP was the same for all three members. The CSIP for the composite I-beam frame members were as follows:

$$\text{CSIP 1} = \begin{bmatrix} [+30]_{16} \\ [\pm 30]_{4s} \\ [+30]_{16} \end{bmatrix}, \quad \text{CSIP 2} = \begin{bmatrix} [+30]_{16} \\ [\pm 30]_{4s} \\ [-30]_{16} \end{bmatrix}.$$

The only difference between the CSIPs of the two beams is in the orientation of the unidirectional plies in the bottom panel of the beam. The in-plane and effective 1-D mechanical properties of the CSIPs are given in Table 1. For the beam considered, $\alpha = 1.65 \times 10^{-2}$ and the critical length was found to be 121 mm. For convenience, a warping superelement length of 100 mm was used, with the non-warping regions divided into lengths of 100 mm. The element stiffness matrix of only a single non-warping element needed to be obtained numerically. It should be noted that even though the length of the critical region is unaffected by the change in CSIP, this change does affect the coupling induced response of the frame. All supports were rigidly fixed. In addition, the ends of Beam 1, Beam 2, and Column 1 were restrained against warping at their common junction. The 1-D model of the framed structure with the load cases is shown in Fig. 3.

For the finite element analysis model used to compare results to the proposed stiffness method analysis, Beam 1, Beam 2 and Column 1 were modeled using 2-D laminated composite general shell elements of quadrilateral shapes "Cquad4" (NASTRAN, 1986). The top, center and bottom panels of Beam 1, Beam 2, and Column 1 were constructed from these elements. A total of 12 elements were used to form each cross-section. Elements

Table 1. Mechanical properties

Property	Laminates $[+30]_{16}$	$[\pm 30]_{4s}$	$[-30]_{16}$
E_1(GPa)	28.78	42.58	28.78
E_2(GPa)	12.48	13.30	12.48
E_6(GPa)	8.76	15.75	8.76
ν_{21}	0.226	0.666	0.226
ν_{12}	0.098	0.203	0.098
ν_{61}	−1.351	0	1.351
ν_{16}	−0.411	0	0.411
ν_{62}	−0.402	0	0.402
ν_{26}	−0.283	0	0.283
$E_{1\text{-D}}$(GPa)	28.78	42.58	28.78
$G_{1\text{-D}}$(GPa)	36.60	15.75	36.60

in the connection region (the junction where Beam 1, Beam 2, and Column 1 meet) were rigidly connected together through the use of rigidlinks, thus effectively restraining the junction against warping. A total of 3600 elements were used. All responses are plotted along the local longitudinal axis (local origin) of Beam 1, Beam 2, and Column 1. The local origins are shown on Fig 2. Results were plotted for the neutral axis nodes (nodes along the midpoint of the center panel), and nodes along the intersections of the top panel/center panel (top flange/web) and center panel/bottom panel (bottom flange/web). To maintain clarity, only angle orientations were indicated in the CSIPs shown in the plots.

Example 1

A moment about the global X-axis $M_x = 1000$ Nmm, was applied at the junction of Beam 1, Beam 2 and Column 1. CSIP 1 is used for the beams and column. Because of the nature of the boundary conditions and loading, six warping superelements were required for this load case, one at each of the three rigid supports and one each at the junction of Beam 1, Beam 2 and Column 1. Thirty non-warping elements were used with a total of 36 elements required for this analysis. Plots of the rotation (total twist) of points along the length of the longitudinal axis of Beam 2 and Column 1 are shown Fig. 4(a) and Fig. 4(b). These are anisotropically induced coupling responses. These responses are not observed in isotropic structures because the coupling terms are not present. Figure 4(c) shows a plot of the rotation (total twist) of Beam 1 due to the load. This response was due to contributions from the twisting moment on Beam 1 and the anisotropic coupling. It can be seen that in all cases the results of the proposed procedure agree very well with results from the finite element analysis (NASTRAN).

Example 2

A transverse force in the global Z-direction $F_z = 500$ N was applied at the center of Column 1. A total of eight warping superelements were required for this load case, one at each of the three rigid supports and at the junction of Beam 1, Beam 2 and Column 1, and two at the load application point in Column 1. Both CSIP 1 and CSIP 2 are analysed. A total of 36 elements were used. Plots of the anisotropic coupling induced rotations (total twist) along the longitudinal axis of Beam 2 [Fig. 5(a) and (b)] and Column 1 [Fig. 5(c) and (d)] are shown for CSIP 1 and CSIP 2. This confirmed the non-uniform response of the structure in the critical regions. Comparing Fig. 5(a) with Fig. 5(b) for Beam 2, and Fig. 5(c) with Fig. 5(d) for Column 1, an interesting phenomenon is observed. No anisotropic coupling induced twist took place in Beam 2 and Column 1 for CSIP 2, whereas coupling induced twist was observed in CSIP 1. This was simply due to the change in the CSIP resulting in changes in the direction of the anisotropic coupling in the flanges. The net effect of the change in direction for CSIP 2 is an out-of-plane displacement without rotation. Figures 5(e) and (f) show the resulting out-of-plane displacement (U_x) of Beam 2 and Column 1 for CSIP 2, respectively. The closeness of the results between the proposed procedure and the finite element analysis is again very evident. Figure 5(g) is a plot of the

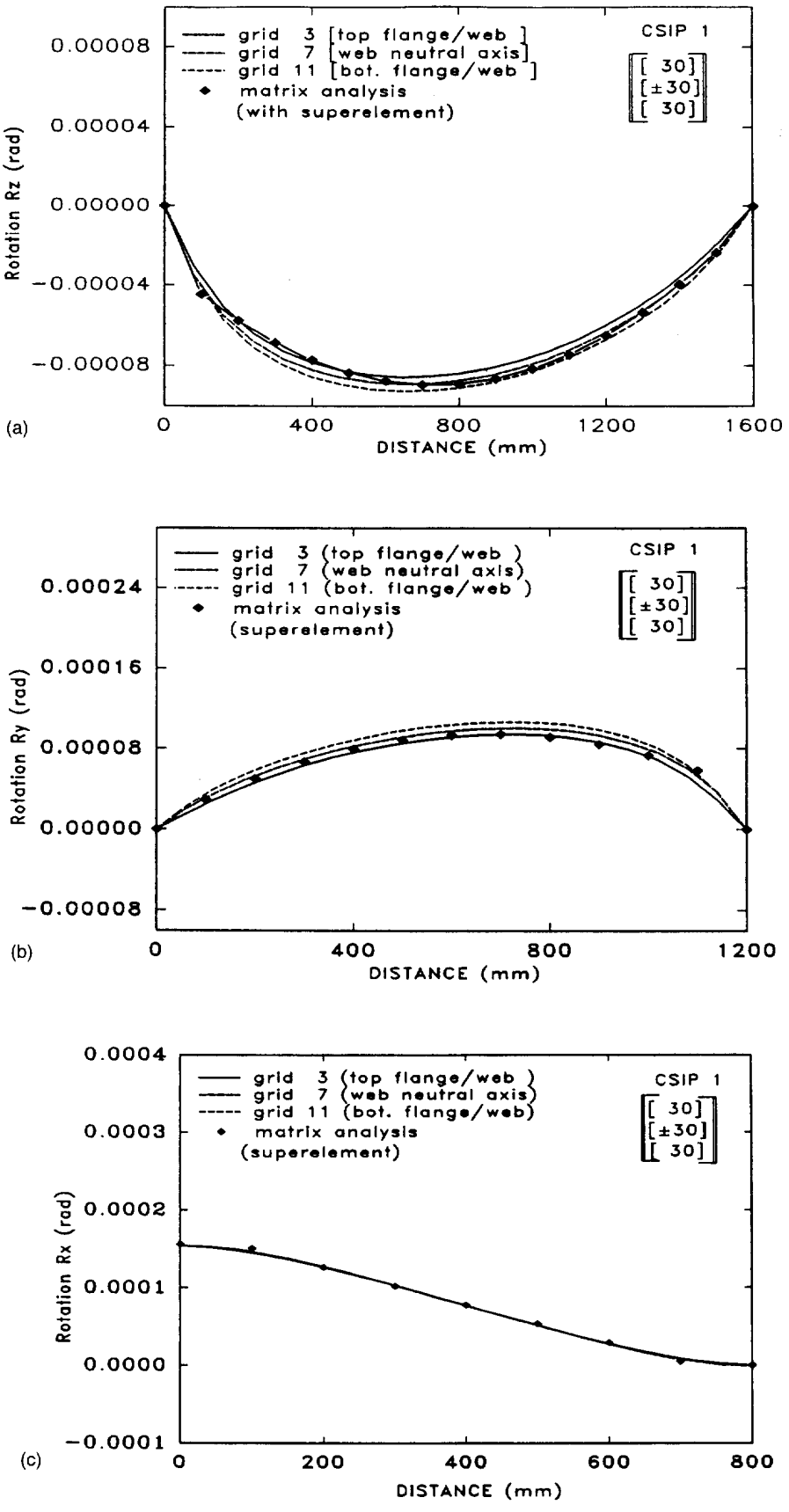

Fig. 4. Example 1 : (a) CSIP 1, rotation of Beam 2 vs distance ; (b) CSIP 1, rotation of Column 1 vs distance ; and (c) CSIP 1, rotation of Beam 1 vs distance.

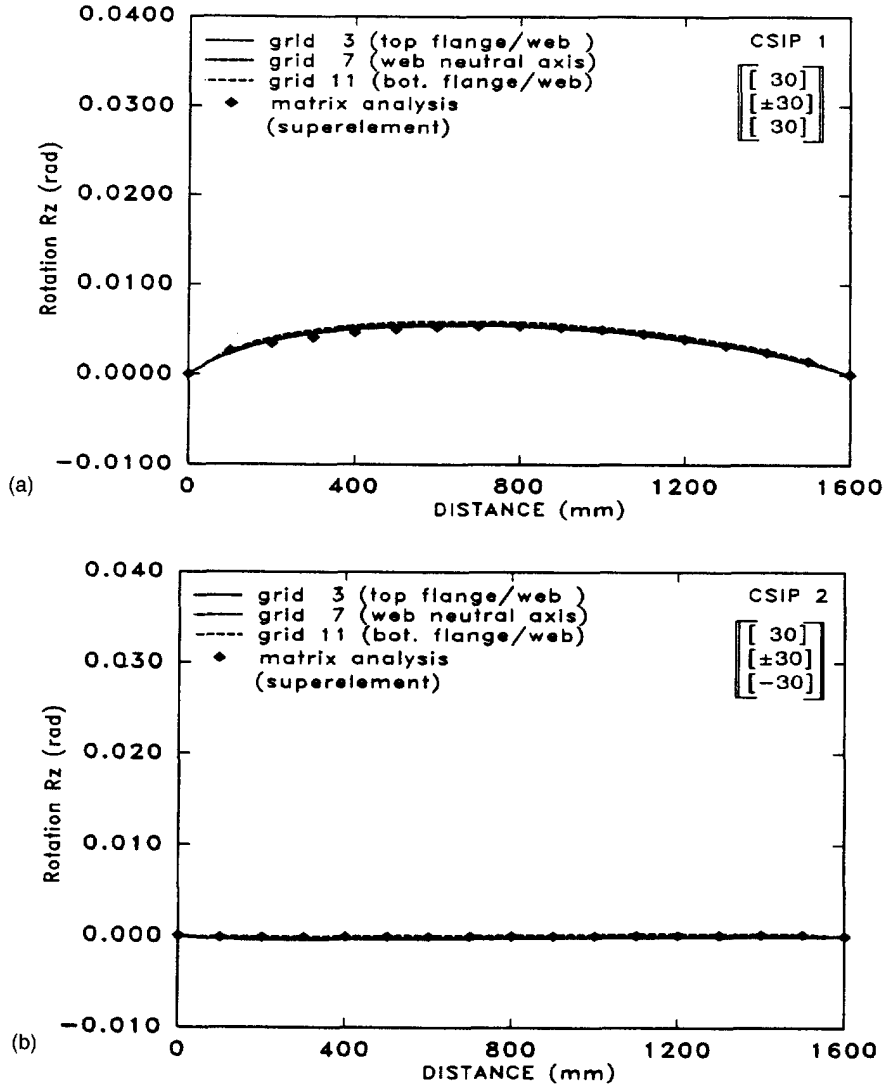

Fig. 5. Example 2: (a) CSIP 1, rotation of Beam 2 vs distance; (b) CSIP 2, rotation of Beam 2 vs distance.

transverse displacement of Beam 2 for CSIP 1. Again the closeness of the result with that of the finite element results can be observed.

DISCUSSION

The above results emphasize the importance of recognizing the existence of anisotropically induced coupling deformations and correctly accounting for them. Furthermore, the potential for utilizing such behavior in design is potentially great if it is well understood. However, one must caution that the possibility of catastrophic failures exit (particularly in dynamic stability and buckling problems) if these effects are not well understood. Torsional responses or torsional-induced coupling responses were primarily shown in the above examples since in the design and analysis of thin-walled structures, combined warping and coupling effects are most significant under torsional load. In isotropic thin-walled structures it is easy to intuitively predict the presence and the direction of the coupled and uncoupled responses. When one deals with anisotropic thin-walled composite structures, one cannot intuitively predict the directions of the coupling induced responses and a complete analysis of the structure is required. The examples demonstrate how sensitive the

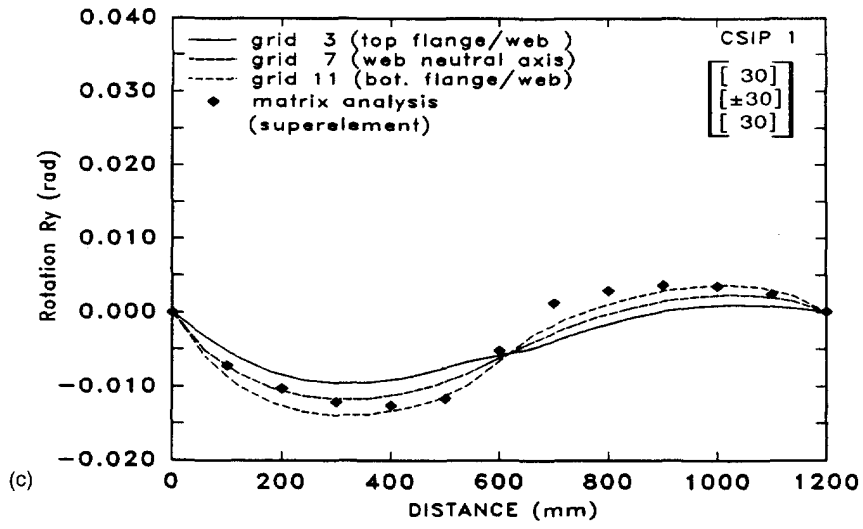

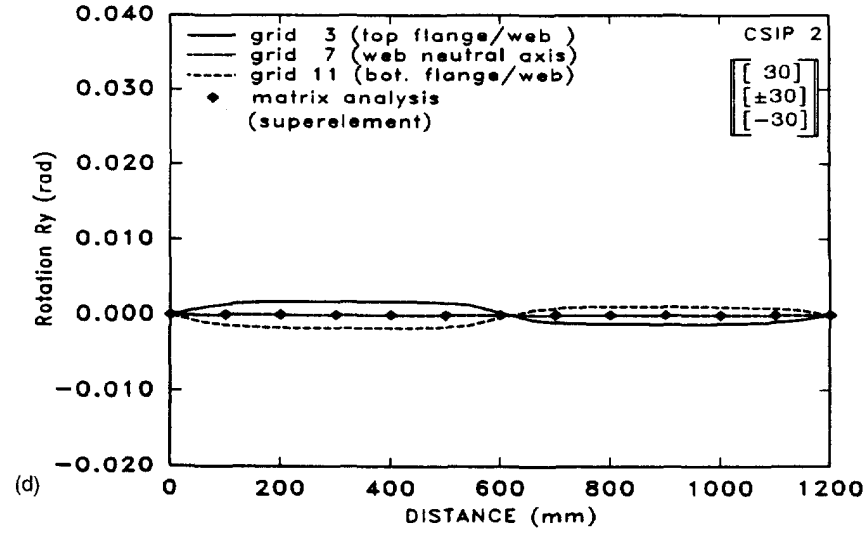

Fig. 5 (*Continued*). (c) CSIP 1, rotation of Column 1 vs distance; (d) CSIP 2, rotation of Column 1 vs distance.

coupling responses are to changes in CSIP. In addition to an intentional change in CSIP in a particular design, a practical situation in which a change in CSIP could occur unintentionally could be during construction or in the analysis. In an anisotropic thin-walled structure such "mistakes" could be fatal.

Another important fact to point out is the computational efficiency of the proposed method. It took only a few seconds on a Unix workstation (Ultrix V4.2A, Dec 5000/133) to perform the analysis of this space frame using the proposed procedure. It took >3 h to perform the same analysis using the Unix version of the NASTRAN finite element package on the Unix workstation, and >72 h using the PC version of NISA-II finite element package on a 386/25 mHz/8 mB RAM computer. Even though additional time was needed for the computation of the effective mechanical and geometric properties and the element stiffness matrices for the warping and non-warping region, the efficiency gained from using a small storage space, coupled with the simplicity of the proposed procedure makes it highly attractive.

CONCLUSION

A one-dimensional 12 d.o.f. beam model for use in the direct stiffness method of the finite element method for analysing anisotropic thin-walled structures has been proposed.

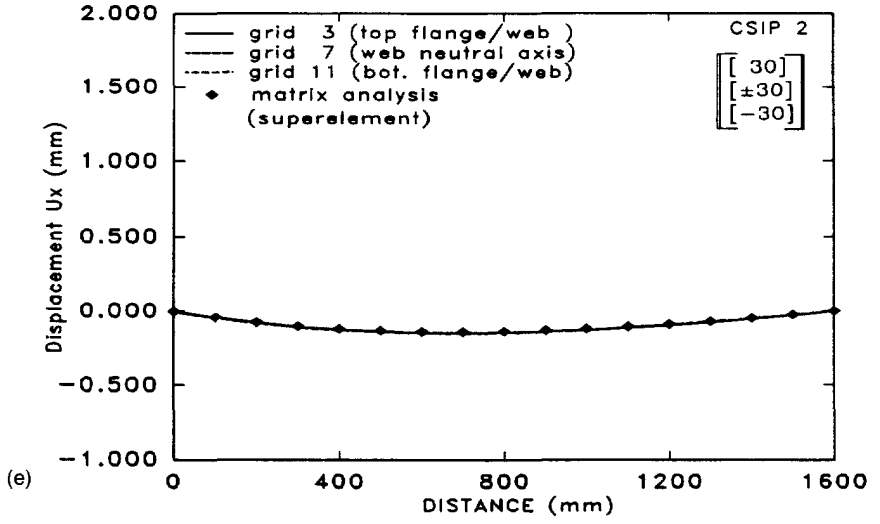

(e)

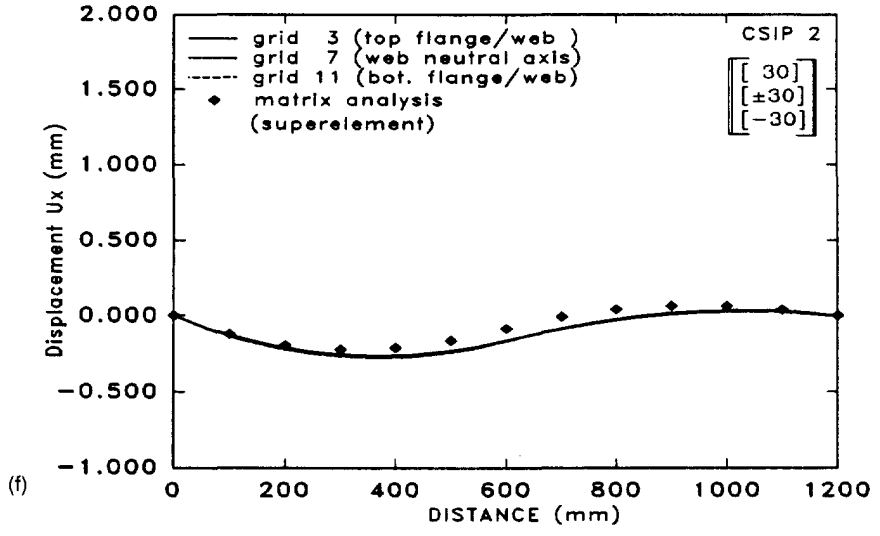

(f)

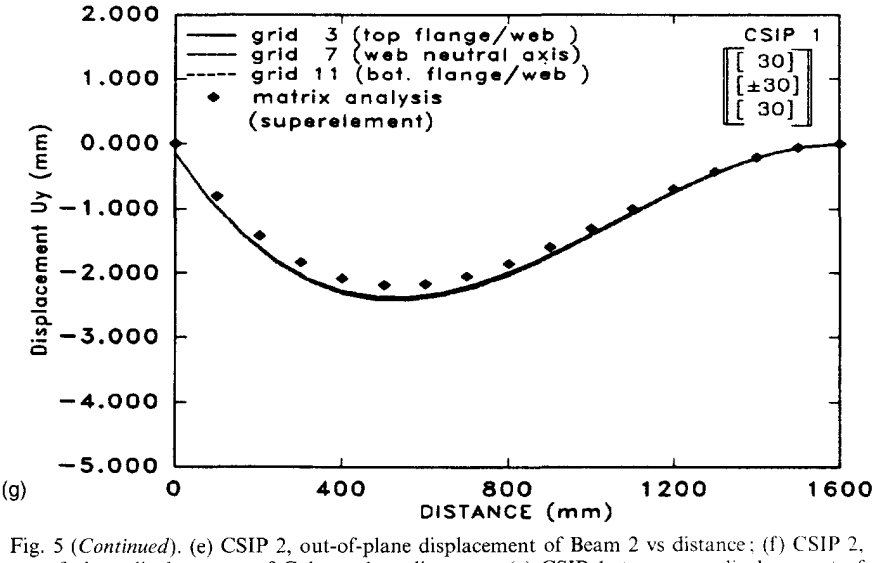

(g)

Fig. 5 (*Continued*). (e) CSIP 2, out-of-plane displacement of Beam 2 vs distance; (f) CSIP 2, out-of-plane displacement of Column 1 vs distance; (g) CSIP 1, transverse displacement of Beam 2 vs distance.

The proposed procedure is simple, accurate and efficient. Only a few elements are required. Warping superelements have been used to specify torsionally restrained conditions without increasing the d.o.f. at the nodes. The numerical technique for developing the stiffness matrices for the warping and non-warping regions of the anisotropic thin-walled beam is accurate and very efficient. Numerical results show good agreement with the finite element analysis. Anisotropic coupling responses have been shown to be significant in thin-walled composite frames. The anisotropic responses are sensitive to changes in composite structural identification pattern. Due to out-of-plane deformations, anisotropic thin-walled structures must always be analysed as 3-D structures.

Acknowledgement—Partial support for this study was provided by the U.S. Army Research Office under contract # DAAL03-G-0084 (Dr Gary Anderson, Program Monitor).

REFERENCES

Bank, L. C. (1990). Modifications to beam theory for bending and twisting of open section composite beams. *Composite Structures* **15,** 93–114.

Bank, L. C. and Cofie, E. (1992). A modified beam theory for bending and twisting of open-section composite beams—Numerical verification. *Composite Structures* **21,** 29–39.

Bank, L. C. and Cofie, E. (1993). Coupled deflection and rotation of anisotropic open-section composite stiffeners. *AIAA J. Aircraft* **30,** 139–141.

Bauld, N. R. and Tzeng, L. S. (1984). A Vlasov theory for fiber-reinforced beams with thin-walled open cross section. *Int. J. Solids Structures* **20,** 277–297.

Chandra, R. and Chopra, I. (1991). Experimental and theoretical analysis of composite I-beams with elastic couplings. *AIAA J.* **29,** 2197–2206.

Cofie, E. (1993a). Finite element analysis of the torsional behavior of thin-walled members using a warping superelement. *Proc. AIAA 34th Structures, Structural Dynamics and Materials Conf.* La Jolla, CA, April 19–22, pp. 292–299.

Cofie, E. (1993b). Analysis of thin-walled isotropic and anisotropic composite structures by the direct stiffness method. Ph.D Dissertation, The Catholic University of America, Washington, DC.

Gjelsvik, A. (1981). *The Theory of Thin-walled Bars*, Wiley, New York.

Gupta, R. K., Venkatesh, A. and Rao, K. P. (1985). Finite element analysis of laminated anisotropic thin-walled open-section beams. *Composite Structures* **3,** 19–31.

Hong, C. H. and Chopra, I. (1986). Aeroelastic stability analysis of a composite bearingless rotor blade. *J. Am. Helicopter Soc.* **31,** 29–35.

Mansfield, E. H. and Sobey, A. J. (1979). The fibre composite helicopter blade, Part 1: stiffness properties, Part 2: prospects for aeroelastic tailoring. *Aeronautical Quarterly* May, 413–449.

Nagarajan, S. and Zak, A. R. (1985). Finite element model for orthotropic beams. *Computers Structures* **20,** 443–449.

NASTRAN Users's Manual (1986). Cosmic Nastran, The University of Georgia, Athens, GA.

NISA Users Manual (1990). NISA-II, Version 90.0, Engineering Mechanics Research Corporation, Troy, MI.

Noor, A. K., Carden, H. and Peters, J. M. (1991). Free vibrations of thin-walled semi-circular graphite–epoxy composite frames. *Int. J. Appl. Finite Elements Computer Aided Eng* **9,** 33–63.

Norris, C. H., Wilbur, J. B. and Utku, S. (1976). *Elementary Structural Analysis*, 3rd Edition, McGraw-Hill Book Company, New York.

Rehfield, L. W. (1985). Design analysis and methodology for composite rotor blades. *7th DoD/NASA Conf. on Fibrous Composites in Structural Design*, Denver, CO, June pp. 1–66.

Sivaneri, N. T. and Chopra, I. (1984). Finite element analysis for bearingless rotor blade aeroelasticity. *J. Am. Helicopter Soc.* **29,** 42–51.

Smith, S. J. and Bank, L. C. (1992). Modifications to beam theory for bending and twisting of open-section composite beams—Experimental verification. *Composite Structures* **22,** 169–177.

Stemple, A. D. and Lee, S. W. (1988). A finite element model for composite beams with arbitrary cross-sectional warping. *AIAA J.* **26,** 1512–1520.

Timoshenko, S. P. and Young, D. H. (1965). *Theory of Structures*, 2nd Edition. McGraw-Hill Book Company, New York.

Tsai, S. W. and Hahn, H. T. (1980). *Introduction to Composite Materials*. Technomic Publishing Company, Inc., Lancaster, PA.

Vinson, J. R. and Sierakowski, R. L. (1987). *The Behavior of Structures Composed of Composite Materials*. Martinus Nijhoff, Dordrecht.

Vlasov, V. Z. (1961). *Thin Walled Elastic Beams*, translated from Russian, published for the National Science Foundation, Washington, DC and the U.S. Dept of Commerce by the Israel Program for Scientific Translation, Jerusalem.

Whitney, J. M. (1987). *Structural Analysis of Laminated Anisotropic Plates*. Technomic Publishing Co. Inc., Lancaster, PA.

Zak, A. R. (1987). Finite element limitations for orthotropic laminated beam analysis. *ASME J. Engng Indus.* **109,** 34–38.